Published in final edited form as:

Cell Signal. 2017 May ; 33: 30–40. doi:10.1016/j.cellsig.2017.02.009.

Enzymatic cleavage of myoferlin releases a dual C2-domain module linked to ERK signalling

Ann-Katrin Piper[a,b], **Samuel E. Ross**[a], **Gregory M. Redpath**[c], **Frances A. Lemckert**[a], **Natalie Woolger**[a,b], **Adam Bournazos**[a], **Peter A. Greer**[d], **Roger B. Sutton**[e,f], and **Sandra T. Cooper**[a,b,*]

[a]Institute for Neuroscience and Muscle Research, Children's Hospital at Westmead, Sydney, NSW 2145, Australia

[b]Discipline of Child and Adolescent Health, Faculty of Medicine, University of Sydney, Sydney, Australia

[c]EMBL Australia Node in Single Molecule Science, School of Medical Science, University of New South Wales, Sydney, NSW, Australia

[d]Department of Pathology and Molecular Medicine, Queen's University, Division of Cancer Biology and Genetics, Queen's Cancer Research Institute, Kingston, ON K7L 3N6, Canada

[e]Department of Cell Physiology and Molecular Biophysics, Texas Tech University Health Sciences Center, Lubbock, TX 79430, USA

[f]Center for Membrane Protein Research, Texas Tech University Health Sciences Center, Lubbock, TX 79430, USA

Abstract

Myoferlin and dysferlin are closely related members of the ferlin family of Ca^{2+}-regulated vesicle fusion proteins. Dysferlin is proposed to play a role in Ca^{2+}-triggered vesicle fusion during membrane repair. Myoferlin regulates endocytosis, recycling of growth factor receptors and adhesion proteins, and is linked to the metastatic potential of cancer cells. Our previous studies establish that dysferlin is cleaved by calpains during membrane injury, with the cleavage motif encoded by alternately-spliced exon 40a. Herein we describe the cleavage of myoferlin, yielding a membrane-associated dual C2 domain '*mini-myoferlin*'. Myoferlin bears two enzymatic cleavage sites: a canonical cleavage site encoded by exon 38 within the $C2_{DE}$ domain; and a second cleavage site in the linker adjacent to $C2_{DE}$, encoded by alternately-spliced exon 38a, homologous

*Corresponding author at: Institute for Neuroscience and Muscle Research, Children's Hospital at Westmead, Sydney, NSW 2145, Australia. sandra.cooper@sydney.edu.au (S.T. Cooper).

Conflict of interest

The author(s) declared no potential conflicts of interest with respect to the research, authorship, and/or publication of this article.

Author's contributions

A. P. designed and conducted the experiments; performed data analysis drafted the manuscript. S. E. R. derived and validated expression constructs, G. I. R. calpain cleavage assays and manuscript editing, F. A. L. assistance and oversight of CRISPR gene editing, N. W. assistance with experimentation and comparison to dysferlin 40a, A. B. assistance with establishing CRISPR gene edited cell lines. P. A. G. provided mouse embryonic fibroblast cell lines, MDA-MB-231 xenograft tumours and editorial revision of manuscript. R. B. S. performed the molecular modelling of the $C2_{DE}$ domain of myoferlin and provided Fig. 3. S. T. C. conceived the initial study, results analysis and interpretation and provided editorial support writing the manuscript.

to dysferlin exon 40a. Both myoferlin cleavage sites, when introduced into dysferlin, can functionally substitute for exon 40a to confer Ca^{2+}-triggered calpain cleavage in response to membrane injury. However, enzymatic cleavage of myoferlin is complex, showing both constitutive or Ca^{2+}-enhanced cleavage in different cell lines, that is not solely dependent on calpains-1 or -2. The functional impact of myoferlin cleavage was explored through signalling protein phospho-protein arrays revealing specific activation of ERK1/2 by ectopic expression of cleavable myoferlin, but not an uncleavable isoform. In summary, we molecularly define two enzymatic cleavage sites within myoferlin and demonstrate 'mini-myoferlin' can be detected in human breast cancer tumour samples and cell lines. These data further illustrate that enzymatic cleavage of ferlins is an evolutionarily preserved mechanism to release functionally specialized mini-modules.

Keywords

Myoferlin; Extracellular-signal-regulated kinase (ERK); Breast cancer; Calpain; Proteolysis; Cell signalling

1. Introduction

Myoferlin is a member of the ferlin family of Ca^{2+}-regulated vesicle fusion proteins [1]. In mammals, there are six ferlins: dysferlin (fer1L1), otoferlin (fer1L2), myoferlin (fer1L3), fer1L4, fer1L5 and fer1L6 [2]. Ferlin proteins have a distinctive structure, with a C-terminal trans-membrane anchor and 5–7 tandem cytoplasmic C2 domains [2], which are Ca^{2+}-regulated lipid and protein binding domains [3]. Proteins that bear C2 domains have varied roles, often involving Ca^{2+}-triggered membrane binding events [4]. The ferlins, synaptotagmins, double C2-like-domain-containing proteins (DOCs), extended synaptotagmin-like proteins and synaptotagmin-like proteins (SLPs) are C2 domain-containing proteins that have been functionally associated with vesicle fusion [5]. Mutations in the dysferlin (*DYSF*) and otoferlin genes (*OTOF*) cause inherited disorders in humans linked to defective vesicle fusion. Mutations in the dysferlin gene cause an inherited late-onset form of muscular dystrophy [6,7], believed to be partially due to defective vesicle fusion required for muscle membrane repair [8]. Mutations in otoferlin cause congenital deafness [9,10], due to defective synaptic exocytosis [11] and vesicle replenishment [12] at the ribbon synapse of the inner ear.

Variants in the myoferlin gene (*MYOF*) have not been implicated in inherited disease, however, emerging evidence links the expression of myoferlin mRNA and protein to the metastatic potential of cancer cells. In breast cancer and renal cell cancer, myoferlin mRNA expression is up-regulated in tumours compared to control tissues [13]. Myoferlin protein levels are upregulated in high-grade pancreatic adenocarcinoma compared to low-grade pancreatic adenocarcinoma or adjacent tissue [14], and myoferlin levels were also elevated in breast ductal adenocarcinoma and breast lobular carcinoma, compared to adjacent control breast tissue [15]. Targeted myoferlin knockdown using siRNA injected into murine tumours grown from Lewis lung cells engrafted into C57BL/ 6 mice reduced tumour size by almost 50% [16]. Furthermore, shRNA-mediated myoferlin knock down in MDA-MB-231 breast

cancer cells was associated with reduced cell migration velocity, and increased cell-matrix and cell-cell interactions *in vitro*, and reduced proliferation and localized invasive behaviour in mouse xenografts [17,18].

Thus, emerging evidence implicates myoferlin in cancer progression and metastasis, with the underlying mechanism still to be elucidated. Several studies show myoferlin regulates growth factor receptor recycling and endocytosis [15,19–22]. Altered growth factor signalling is linked to the progression and pathogenesis of different carcinoma types [23,24], and tumours often secrete autocrine acting growth factors [25]. Given the established roles of ferlin proteins in dynamic membrane remodelling, including endocytosis and secretion, it is plausible that myoferlin regulates signalling events in cancer cells that contribute to proliferation and metastasis.

Our previous studies demonstrate that dysferlin is cleaved by calpains-1 and -2 in response to the Ca^{2+} influx caused by membrane injury. Calpain cleavage of dysferlin releases a C-terminal fragment of ~72 kDa, mini-dysferlin$_{C72}$, bearing two C2 domains anchored by the transmembrane domain, with broad structural homology to the synaptotagmin family of vesicle fusion proteins [26,27]. As antibodies directed against N-terminal epitopes are unable to detect dysferlin at injuries sites, data suggest the C-terminal mini-dysferlin$_{C72}$ is the species recruited to sites of membrane injury, where it may function as a specialized membrane repair module [26,27]. Our previous studies also demonstrated other ferlin paralogues could be cleaved by calpains *in vitro* [27].

Our interest in myoferlin was piqued by reports showing myoferlin as a doublet band in western blots when detected with N-terminal epitope specific antibodies [16,28–30]. This was reminiscent of the N-terminal calpain-cleavage fragment we reported for dysferlin [26,27]. Herein, we provide evidence that myoferlin is also proteolytically cleaved in breast cancer tumours and cell lines, releasing a C-terminal ‘mini-myoferlin’ fragment. We molecularly characterize two myoferlin cleavage sites in close proximity at the fifth C2 domain, C2$_{DE}$ (between C2$_D$ and C2$_E$, and not annotated by PFAM and/or SMART for all ferlin paralogues). Further we show that ectopic expression of the cleavable canonical myoferlin isoform, but not an uncleavable isoform, leads to increased ERK1/2 phosphorylation (extracellular signal–regulated kinase), providing a potential connection between myoferlin cleavage and the MAPK/ERK pathway linked to cancer cell progression.

2. Material and methods

2.1. Cell culture

HEK293 and MO3.13 cells were cultured in DMEM (Life Technologies) containing 10% FBS (Life Technologies). COS-7 and MEF cells were cultured in 1:1 DMEM:F12 (Life Technologies) containing 10% FBS. EVSA-T cells were cultured in MEM + 1xNEAA (non-essential amino acids) containing 10% FBS, MCF-7, BT-474 and MDA-MB-231 cells were cultured in RPMI 1640 (Life Technologies) containing 10% FBS. All media contained 50 μg/mL gentamicin (Life Technologies). Cells were harvested by scrape injury as described in Lek et al., 2013 [26].

2.2. SDS-PAGE and western blotting

Procedures were performed as described in [27].

2.3. Transfection

HEK293 cells were transfected using PEI (polyethylenimine Max, Polysciences) and COS-7 with Lipofectamine® LTX (LifeTechnologies) as described in [27].

2.4. Immunoprecipitation

Epitope-tagged ferlin constructs were immunoprecipitated from transfected HEK293 cells using anti-Myc antibody following the protocol described in [27].

2.5. In vitro calpain cleavage

Purified calpain-1 (porcine) and -2 (human) were purchased from Millipore. *In vitro* cleavage of the ferlin proteins was performed using a modified protocol from Mandic et al. [31]. Protein G–Sepharose–bound ferlin proteins were washed three times in 20 mM 4-(2-hydroxyethyl)-1-piperazineethanesulfonic acid (Sigma-Aldrich; pH 7.5), 50 mM NaCl, and 1 mM $MgCl_2$ containing 2 mM $CaCl_2$. Diluted recombinant calpain was added directly to the protein G–Sepharose–bound ferlin proteins and incubated at 30 °C for 10s. and 2 min. as indicated. Digestion was quenched by reconstitution into 2× SDS loading buffer (4% SDS, 20% glycerol, 125 mM Tris, pH 7.4, and 10 mM DTT (Sigma-Aldrich)), and samples were heated to 94 °C for 3 min.

2.6. In vitro cathepsin L cleavage

Protein bound sepharose beads were transferred into trisacetate cleavage buffer (50 μL for each experimental condition) and split evenly into one tube for each condition used. 10 ng/μL purified recombinant human cathepsin L (952-CY, R&D systems) diluted in trisacetate buffer on ice was added to ferlin-bound Protein-G beads and incubated for the indicated time at 30 °C. Method adopted from Goulet et al., 2004 [32]. Afterwards samples were handled like described under *in vitro* calpain cleavage.

2.7. Proteome profiler

We have used the Proteome Profiler Human Phospho-MAPK (ARY002B) and the Mouse-RTK Array Kit (ARY014) from R&D systems and followed the company's instructions.

2.8. Antibodies

Antibodies used in western blotting included N-terminal anti-myoferlin (7D2, α-rabbit, 1:2000 abcam, ab76746, lot# GR209175-4), C-terminal anti-myoferlin (K16, α-goat, 1:200; Santa cruz, sc-51,367, lot# A6714), C-terminal anti-dysferlin (Hamlet-1, α-mouse, 1:5000; Leica Microsystems, Wetzlar, Germany, NCL-Hamlet, lot# 6045527), N-terminal anti-dysferlin (Romeo, α-rabbit, 1:1000; abcam, ab124684), mid region anti-dysferlin, (Fer-A, α-rabbit, 1:1000; Sigma-Aldrich, HPA021945, lot# R10883), anti-Myc (α-rabbit, 1:5000; abcam, ab9106, lot# GR130480-24), anti-β-tubulin (1:1000; Developmental Studies Hybridoma Bank, E7-c 8 M4, lot# 4/16/15), anti-GAPDH (α-mouse, 1:10,000; Merck, Millipore, MAB374, lot# 2742734), anti-FLAG M2 (α-mouse, 1:5000, Sigma Aldrich,

F3165, lot# SLBH1191V), anti-phosphoERK1/2 (α-rabbit, 1:1000, P-p44/42 (T202/Y204) MAPK, Cell signaling, 4370P, lot#17), anti-ERK (α-rabbit, 1:1000, p44/42 MAPK ERK1/2, Cell Signalling, 4695P, lot#14), anti-phosphoAKT (α-rabbit, 1:1000, Cell signaling, (Ser473), 9271S, lot# 9), anti-CAPNS1 (Calpain reg (P1), α-mouse, 1:500, Santa cruz, sc-32325, lot# E0907). For all these antibodies membranes were blocked in 5% skim milk in PBS + 1% tween (for K16 block in 1% skim milk in PBS-T and probe with 5% BSA in PBS-T). For anti-Calpain-2 (Large subunit (M-type), α-rabbit, 1:1000, Cell signaling, 2539S, lot# 2) and anti-Calpain-1 (1:500, α-goat, Santa cruz, sc-7531, lot# L0209) use 5% BSA for block and antibody dilution.

2.9. PCR and primers

Polymerase chain reaction (PCR) was carried out on human cDNA panels purchased from Clontech (Mountain View, CA; Human MTC Panel I and Human Immune MTC Panel). Primers to myoferlin 5″ GCCTCCCTTCTGTCTGCCCCAC 3″ and 3″ GTCAGGCCCTCAAATTCTGC 5″. GAPDH primers were supplied as part of the Clontech cDNA panel kit.

2.10. Constructs

The dysferlin cDNA construct (EGFP-FL-DYSF pcDNA3.1, National Center for Biotechnology Information [NCBI] reference sequence NP_003485.1) was a generous gift from Kate Bushby (Institute of Human Genetics, International Centre for Life, Newcastle upon Tyne, UK), and was subcloned into pIRES2-EGFP (OriGene). Myoferlin-pCMV6 (NCBI reference sequence NM_013451.3) was purchased from OriGene (Rockville, MD) and subcloned into pIRES2-EGFP. Exon 38a–containing constructs (M_{38a}, NCBI reference sequence sp|Q9NZM1-3) were generated by PCR amplification of exon 38a from human lung cDNA. Exon 38a-containing products were isolated and digested with *Pst*I and *Sac*I (New England Bioscience, Ipswich, MA) and inserted into our *Pst*I/*Sac*I digested FL-MYOF-pIRES2 construct. All constructs were validated by DNA sequencing.

2.11. Protein alignment and calpain cleavage prediction

Protein alignment was performed using ClustalW [33]. Calpain cleavage prediction was performed using GPS-CCD (ccd.biocuckoo. org; [34]).

2.12. Homology modelling

The 3D model of myoferlin $C2_{DE}$ was done using Modeller [35]. The $C2_{DE}$ primary sequence (residues 1263–1393 of human myoferlin; GENBANK: AAF27177.1) was aligned with the primary sequence of myoferlin $C2_A$, and used to compute a 3D model of the domain. The 3D model was based on coordinates deposited in the PDB database using the NMR structure of myoferlin $C2_A$ (2DMH) as a template. Ten representative models were calculated. The model with the lowest energy score was used for analysis.

2.13. Statistics

Statistics was performed using Prism 6 (GraphPad) using Ordinary one-way ANOVA for analysis of proteome profiler arrays relative to pIRES.

3. Results

3.1. Myoferlin cleavage products are detected in breast tumours, breast cancer cell lines and transfected cells

Based on published reports demonstrating a doublet band for myoferlin in cells and tissues [16,28,29], and our own data showing the canonical myoferlin isoform (Q9NZM1) may be cleaved enzymatically in transfected HEK293 cells [27], we sought to define the molecular determinants of myoferlin cleavage.

We detected an N-terminal myoferlin cleavage product in mouse xenograft tumours established using the human triple negative breast cancer cell line MDA-MB-231 (Fig. 1A), confirming cleaved myoferlin is present in cancerous tissues. In cultured MO3.13 human oligodendrocytic cells, the N-terminal cleavage product appeared only in the presence of extracellular Ca^{2+} and membrane injury, whereas in C2C12 cells, the cleavage product was also seen in resting cells (Fig. 1A).

Western blot analyses of two human breast tumours and four human breast cancer cell lines (BT-474, EVSA-T, MCF-7 and MDA-MB-231 cells) confirmed evidence for C-terminal fragments of ~75 kDa (detected by the C-terminal antibody K-16, Fig. 1B), as well as an N-terminal counter fragment of ~160 kDa (detected by 7D2, Fig. 1B). In breast cancer cell lines, levels of the cleaved C-terminal fragment were elevated acutely (within 2 min) using a scrape assay that induces membrane injury and acute Ca^{2+}-flux. The two human tumour samples were aggressive triple negative breast cancers, with the corresponding hematoxylin and eosin staining representing the tumour content from each sample (Fig. 1C, samples #88 ~50% tumorous and #89 ~75% tumorous). Mini-myoferlin is detected as a doublet with the dominant band detected at a slightly lower apparent molecular weight compared to an MDA-MB-231 control. The counter fragment appears to be of similar size between tumour samples and the MDA-MB-231 control.

Transfection studies in COS-7 and HEK293 cells with myoferlin (Q9NZM1), isoform 1, (the canonical myoferlin isoform) compared to dysferlin 40a (isoform containing exon 40a and the calpain cleavage site) revealed clear differences in Ca^{2+}-triggered formation of the cleavage products in the different cell lines (Fig. 1D). In HEK293 cells, cleaved fragments of myoferlin were detected in resting cells that had not been subject to a membrane injury and Ca^{2+}-flux (Fig. 1D). Whereas, in COS-7 cells, only low levels of the cleavage products were detected in resting cells, with cleavage activated by scrape injury in the presence of extracellular Ca^{2+} (Fig. 1D).

These studies highlight significant differences between proteolytic cleavage of myoferlin and dysferlin. Dysferlin shows strict injury- and Ca^{2+}-dependent cleavage by the ubiquitous calpain-1 and/or -2, with the proteolytic cleavage site refined to residues encoded by the alternately spliced exon 40a [27]. These data reveal that the canonical myoferlin isoform (Q9NZM1) myoferlin is also cleaved enzymatically, but shows different requirements for Ca^{2+} in different cell lines.

3.2. Myoferlin bears two proteolytic cleavage sites

In silico analyses of myoferlin using a calpain cleavage prediction program (GPS-CCD, ccd.biocuckoo.org [34]) identified two high confidence calpain cleavage sites (Fig. 2A) that could produce C-terminal cleavage products matching the ~75 kDa of our observed mini-myoferlin. The first site is encoded by exon 38 (SLLS|APPC) within the fifth C2 domain ($C2_{DE}$), and is present in all myoferlin isoforms (Fig. 2B). The second site, encoded by alternatively spliced exon 38a (SKMA|SPAT), would be located 34 residues C-terminal to the first site in the $C2_{DE}$ domain (in exon 38) (Fig. 2B). Phylogenetic alignments revealed that alternately spliced myoferlin exon 38a is conserved in vertebrates, from humans through to the fish class (Fig. 2C). Alignment of myoferlin sequences to human dysferlin demonstrates the predicted cleavage site in myoferlin exon 38a aligns with the known cleavage site in dysferlin exon 40a (Fig. 2C). PCR analysis of a human cDNA panel (Clontech Multiple Tissue cDNA panels I and II) revealed that transcripts including exon 38a are a minor species (~10–15% of all transcripts) in all analyzed tissues (Fig. 2D). This conservation of alternative exons in the identical positions in dysferlin and myoferlin argues that its origin predates ferlin gene expansion in early chordates [2].

3.3. Molecular modelling of the cleavage sites in myoferlin

We modelled the first putative calpain cleavage site in myoferlin encoded by exon 38 (present in all isoforms) using the solved crystal structure of the $C2_A$ domain of myoferlin as the homology model for myoferlin $C2_{DE}$, as it is the most similar C2 domain currently solved (Fig. 3A). C2 domains fold dynamically in response to binding of Ca^{2+} and phospholipids, therefore structural modelling of $C2_{DE}$ allowed us to query whether accessibility of the cleavage motif may be regulated by the conformational structure of the $C2_{DE}$ domain. For example, if a predicted cleavage site mapped to residues of a β-strand contributing to the hydrophobic core of the C2 domain, enzymatic cleavage may be precluded when the domain is folded. Homology modelling indicates the first cleavage site (encoded by exon 38) is located in a loop between the last two beta strands (β7 and β8) of myoferlin $C2_{DE}$ (red loop, Fig. 3A). Thus, in this case, it is theoretically plausible this putative calpain-cleavage site may be cleaved enzymatically whether or not the $C2_{DE}$ domain is folded. Interestingly, alignment of residues predicted to comprise the $C2_{DE}$ domain of dysferlin and myoferlin reveal very high amino-acid identity, *except* for this region encompassing the last two beta strands and loop (Fig. 3B, β7 and β8). Importantly, the canonical dysferlin isoform-1 (O75923) cannot be cleaved by calpains [27], consistent with these non-homologous residues in myoferlin encompassing a predicted novel calpain cleavage site not present in dysferlin.

The second putative calpain cleavage site encoded by alternatively spliced exon 38a is immediately adjacent to the $C2_{DE}$ domain, in the linker region between $C2_{DE}$ and $C2_E$ (Fig. 3A, dashed line, yellow represents cleavage site).

3.4. Both predicted calpain cleavage sites in myoferlin can functionally confer Ca^{2+}-dependent, calpain-cleavage of dysferlin

To determine whether the two predicted calpain cleavage sites in myoferlin represent bonafide calpain cleavage sites, we created a series of chimeric constructs (see Fig. 4A and

B). We reciprocally substituted residues encompassing the first putative calpain cleavage site within the myoferlin $C2_{DE}$ domain (encoded by exon 38), with the analogous residues of the dysferlin $C2_{DE}$ domain (encoded by exon 40), that we have shown experimentally is not cleaved by calpains [27]. We used data derived from structural modelling and amino acid sequence homology to precisely substitute residues comprising the 7th and 8th β-strands and intervening loop, that bear the putative cleavage motif (SLLS|APPC) in myoferlin with the corresponding dysferlin region (constructs D_{M38} and M_{D40}, see Fig. 4A and B). To test whether the second putative myoferlin cleavage site encoded by alternatively-spliced myoferlin exon 38a was functionally analogous to dysferlin exon 40a, we created a myoferlin expression construct bearing exon 38a encoded sequences (M_{38a}), and, in the dysferlin backbone, we substituted dysferlin exon 40a, with myoferlin exon 38a (D_{M38a}). We performed *in vitro* calpain cleavage assays using recombinant calpain (Fig. 5A), as well as "in cell" cleavage assays in HEK293 cells overexpressing each construct (Fig. 5B).

Myoferlin and dysferlin proteins were immunoprecipitated from transfected HEK293 cell lysates with an anti-Myc antibody and protein-G-sepharose, then exposed to recombinant calpain-1 or -2 (calpain-2 not shown) (Fig. 5A, left panel). Full-length dysferlin (D_{FL}) that lacks exon 40a served as a negative control, as it does not encode for a calpain cleavage site, and thus shows no detectable cleavage products (Fig. 5A and B left panels. Also see [27]). As expected, dysferlin bearing exon 40a (D_{40a}) is cleaved effectively by recombinant calpain, releasing C-terminal mini-dysferlin (Fig. 4A, left panel, anti-Myc blot) and the N-terminal counter fragment (Fig. 5A, left panel, Romeo blot). Substitution of sequences encoding either predicted myoferlin cleavage sites in dysferlin (D_{M38} or D_{M38a}) revealed both sites are cleaved by calpains *in vitro* (Fig. 5A). Similarly, both myoferlin cleavage sites are cleaved in a Ca^{2+}-dependent manner in transfected HEK293 cells subjected to scrape injury, analogous to dysferlin exon 40a (Fig. 5B, left panel, D_{M38} and D_{M38a}).

Thus, both *in vitro* and 'in cell' cleavage assays confirmed *in silico* predictions of myoferlin exon 38 encoded residues SLLS|APPC as a calpain cleavage motif. Full-length myoferlin (M_{FL}) is cleaved by calpains *in vitro* (Fig. 5A, right, M_{FL}), and is cleaved constitutively in transfected HEK293 cells without membrane injury and Ca^{2+}- flux (Fig. 5B, right, M_{FL}). Conversely, substitution of the canonical myoferlin exon 38 site with homologous dysferlin exon 40 (uncleavable) residues strongly reduced formation of cleavage products (Fig. 5A and B, right, M_{D40}), consistent with previous evidence demonstrating these dysferlin sequences are not a favoured calpain cleavage site [27].

More complex results were obtained using myoferlin constructs to study the second exon 38a encoded site that is homologous to the dysferlin cleavage motif within alternative exon 40a. Surprisingly, myoferlin bearing exon 38a (M_{38a}), which now possesses both predicted calpain cleavage sites, was not cleaved *in vitro* or in transfected HEK293 (Fig. 5A and B, right panels, M_{38a}). Interestingly, when the canonical myoferlin exon 38 site is replaced by the homologous 'uncleavable' dysferlin exon 40 sequence, and exon 38a is the only potential cleavage site ($M_{D40/38a}$), the capacity to be cleaved by calpains is restored, in both *in vitro* and 'in cell' cleavage assays (Fig. 5A and B, right, $M_{D40/38a}$). Thus, inclusion of exon 38a sequences in myoferlin blocks the capacity of myoferlin protein synthesized in HEK293

cells to be cleaved at the canonical exon 38 site '*in cells*' or *in vitro* by purified recombinant calpain.

3.5. Myoferlin cleavage is independent of calpain-1 and -2 in cells and the cleavage modality is dictated by the C-terminus

To establish if calpain-1 and/or -2 were responsible for enzymatic cleavage of myoferlin, we performed targeted knock out of the calpain small subunit 1 (CAPNS1) in HEK293 cells, an approach that renders calpain-1 and -2 inactive and leads to the secondary reduction/ablation of the CAPN1 and CAPN2 proteins [36]. Canonical myoferlin (M_{FL}) was cleaved effectively in HEK293 cells lacking CAPNS1 (Fig. 5B right panel), whereas the cleavage of dysferlin 40a (D_{40a}) was ablated in the absence of CAPNS1.

To understand why myoferlin and dysferlin display different cleavage patterns, we sought to determine whether features intrinsic to this C-terminal region play a role in conferring constitutive or Ca^{2+}- dependent cleavage. Our phylogenetic studies establish the two C-terminal C2 domains of ferlins are the most evolutionarily conserved, implying a core function [2]. We generated another chimeric construct, precisely substituting the C-terminal 'mini-myoferlin' module with the equivalent mini-dysferlin sequences (M_{mDf}, Fig. 6A; dashed line indicates where the sequences have been swapped over). Interestingly, a myoferlin construct with a dysferlin C-terminal domain now behaves like dysferlin, displaying Ca^{2+}- and injury-dependent cleavage. Ca^{2+}- and injury-dependent cleavage of the M_{mDf} chimera was also greatly attenuated in *CAPNS1*$^{-/-}$ HEK293 cells, in line with its dysferlin-like properties (Fig. 6B).

Taken together, these observations argue that Ca^{2+}-triggered proteolytic cleavage by calpain-1 or calpain-2 is conferred by the mini-dysferlin sequences. Furthermore, these results establish that an enzyme other than calpain-1 and/or -2 is responsible for Ca^{2+}- and injury-independent cleavage of myoferlin. In support of this, endogenous myoferlin cleavage was also observed in mouse embryonic fibroblasts (MEFs) derived from either WT or CAPNS1 KO mice (Fig. 6C). With the cleavage occurring in resting cells independent of Ca^{2+} and membrane injury (Fig. 6C). The cathepsin family of lysosomal proteases is also predicted to cleave myoferlin at the same amino acid sequence as calpains are (SLLS| APPC). In an *in vitro* cleavage assay cathepsin L released the same-sized mini-myoferlin fragment as calpains (Fig. 6D).

3.6. Cleaved myoferlin increases ERK phosphorylation in HEK293 cells

As myoferlin is known to play a role in growth factor receptor recycling and secretion [15,19–22], we used proteome profiler arrays to investigate the effects of our cleavable and uncleavable myoferlin constructs on the relative phosphorylation of 65 proteins implicated in receptor tyrosine kinase (RTK) and mitogen-activated protein kinase (MAPK) signalling pathways (Phospho-RTK Antibody Array and Phospho-MAPK Antibody Array from R&D Systems). We overexpressed myoferlin full-length (M_{FL}), myoferlin 38a (M_{38a}), dysferlin full-length (D_{FL}) and vector only control (pIRES2-EGFP) in HEK293 cells. Interestingly, phosphorylated ERK1 and -2 were specifically increased with overexpression of full-length myoferlin, but not when myoferlin 38a, dysferlin or pIRES2 vector control was

overexpressed (Fig. 7A shows the results of 13 representative proteins). We validated these results by conventional western blot analyses using different phospho-ERK1/ 2 antibodies (Cell Signaling). Three separate experiments were performed for myoferlin (Fig. 7B) and two for dysferlin (Fig. 7C) in triplicate repeats that demonstrate a two-fold increase in phospho-ERK1/2 when myoferlin FL is transfected, relative to pIRES2 vector control (Fig. 7D). As ~30–40% cells were transfected (shown by flow cytometry using the EGFP expressed from the internal ribosome entry site in pIRES2, (data not shown)), the upregulation in transfected cells would likely exceed the biochemically observed average of 2-fold. This effect was specific to ERK phosphorylation and did not alter the phosphorylation status of AKT, a downstream target of the PI3 kinase-signalling pathway (Fig. 7B). These data demonstrate reproducible, differential activation of pERK with canonical myoferlin, but not myoferlin$_{38a}$, which is identical with the exception of 57 base pairs encoded by exon 38a. Although further research is required to determine the functional relevance of myoferlin cleavage, these data support functional specialisation conferred by alternate myoferlin isoforms and linked to enzymatic cleavage.

4. Discussion

In this study we molecularly characterize two enzymatic cleavage sites within myoferlin in close proximity at the fifth C2 domain, C2$_{DE}$. When either of the myoferlin cleavage sites are expressed in a dysferlin expression construct, both exon 38 and exon 38a cleavage motifs can functionally substitute for dysferlin exon 40a sequences to confer Ca^{2+}-dependent and calpain-dependent cleavage of dysferlin in response to injury. Enzymatic cleavage of endogenous myoferlin expressed in breast cancer lines, MO3.13 oligodendroglial cells and in transfected COS-7 cells is enhanced following acute Ca^{2+} flux induced by membrane injury, suggesting cleavage of myoferlin is activated by Ca^{2+}-signalling. However, in primary mouse embryonic fibroblasts, C2C12 mouse myoblasts and transfected HEK293 cells, release of myoferlin cleavage products occurred in resting cells.

These data suggest different signalling pathways and different enzymes regulate myoferlin cleavage in different cells and tissues, but did not exclude that enzymatic cleavage of both dysferlin and myoferlin was linked to Ca^{2+}-signalling and calpain activation. Calpain-1 can be activated by intracellular Ca^{2+} concentrations (EC_{50} ~20 μM), whereas calpain-2 has a much higher activation threshold and has an EC_{50} ~200μM Ca^{2+} [37]. Calpain-2 can also be activated *via* kinase-mediated phosphorylation through epidermal growth factor receptor signalling in a Ca^{2+}-independent manner [38–40]. However, targeted knockout of CAPNS1 in HEK293 and MEF cells demonstrated the ubiquitous calpains, calpain-1 and -2, are not responsible for enzymatic cleavage of myoferlin.

There are 15 members of the calpain family [41] and the lysosomal cathepsins also share overlapping substrate specificities to calpains. Lysosomal cathepsins are Ca^{2+}-independent proteases that are active at slightly acidic pH and rapidly inactivated by neutral pH [42]. The myoferlin exon 38 motif (SLLS|APPC) registered as a likely cathepsin substrate *via in silico* predictions (ExPasy), and recombinant cathepsin L readily cleaved myoferlin *in vitro* to release similar cleavage products as observed with recombinant calpain (see Fig. 6D).

Cathepsins make attractive candidates for myoferlin cleavage, as they are highly expressed in invasive tumours [43].

Paradoxically, in transfected HEK293 cells inclusion of the second myoferlin cleavage motif encoded by alternately spliced exon 38a blocks enzymatic cleavage at the canonical exon 38 site, both in the '*in cell*' and the '*in vitro*' cleavage using recombinant calpain. These results suggest inclusion of exon 38a sequences may induce a change in tertiary conformation, or promote a post-translational modification or interaction (preserved following immunoprecipitation), that prevents enzymatic cleavage. Alternately, it is plausible myoferlin is cleaved and the released products are labile. Other proteins are known to have two different enzyme cleavage sites very close together, including α-spectrin [44,45] and α-fodrin [46], whereby cleavage by caspases or calpains release similarly sized products in response to different cellular triggers. For example, calpain cleavage of α-fodrin can occur during platelet activation [47,48] whereas caspase cleavage of α-fodrin is linked to apoptosis [49]. Inclusion of exon 38a in myoferlin may confer preferential enzymatic cleavage by an enzyme not present in the cellular systems of our studies.

To try to identify domains that bestow calpain/Ca^{2+}-*dependent* cleavage on dysferlin, but calpain/Ca^{2+}-*independent* cleavage on myoferlin in transfected HEK293 cells, we studied a myoferlin-dysferlin chimera. These experiments revealed that 'dysferlin-like' properties are conferred to myoferlin through substitution of the myoferlin C-terminus with the dysferlin C-terminus (mini-dysferlin$_{C72}$). Interestingly, this dual-C2 domain module is highly conserved between dysferlin and myoferlin, with 60% amino acid identity (ExPasy). The different properties of enzymatic cleavage between dysferlin and myoferlin in transfected HEK293 may reflect intrinsic differences in Ca^{2+}- or lipid- binding preferences of the $C2_E$ and $C2_F$ domains, and/or differences in the cellular journey of dysferlin and myoferlin dictated by this C-terminal region that exposes each protein to different enzymes. Dysferlin and myoferlin do not have overlapping functional roles, as shown by the inability of myoferlin to functionally compensate for dysferlin-deficiency in dysferlin-null mice [50].

To obtain clues to the functional consequences of myoferlin cleavage, we performed phosphorylation profiling of 65 signalling proteins. Overexpression of 'cleavable' myoferlin (without exon 38a) consistently resulted in increased phosphorylation of ERK1/2 (Fig. 7). MAPK/ERK signalling is implicated in cell growth, adhesion, cell survival and differentiation, and its inappropriate activation has been linked to different carcinoma types [51]. Our ongoing studies will explore the consequence of myoferlin over-expression on MAPK/ERK signalling pathways in a transgenic mouse model, to better elucidate the functional consequences of myoferlin cleavage and its potential relationship to growth factor receptor signalling and the metastatic properties of cancer cells. Enzymatic cleavage of myoferlin may explain detection of myoferlin as a 240/170 kDa N-terminal doublet band in tumour samples and cancer cell lines in recent reports describing a role for myoferlin in tumorigenesis and cancer cell metastasis [16,28–30], potentially illuminating a functional adaptation of myoferlin relevant to cellular signalling and oncogenesis.

5. Conclusions

- Myoferlin can be cleaved enzymatically *via* both calpain-dependent and calpain-independent mechanisms to release a dual C2 domain transmembrane-anchored module.
- Myoferlin bears two enzymatic cleavage sites; a canonical cleavage site encoded by exon 38 within the $C2_{DE}$ domain; and a second cleavage site in the linker adjacent to $C2_{DE}$, encoded by alternately-spliced exon 38a, homologous to dysferlin exon 40a.
- Differential activation of ERK signalling with *in vitro* overexpression of cleavable myoferlin, but not uncleavable myoferlin, supports functional specialisation conferred by alternate myoferlin isoforms and linked to enzymatic cleavage.
- Enzymatic cleavage of both dysferlin and myoferlin infers evolutionary preservation of a means to release dual C2 domain modules; perhaps an ancestral prototype of synaptotagmin-like effectors.

Acknowledgments

This work was supported by the Australian National Health and Medical Research Council (Project Grant APP1048814 to S.T.C.; Career Development Fellowship APP1048816 to S.T.C.), the Jain Foundation (S.T.C.), the University of Sydney Australian Postgraduate Awards (N.W., and A.K.P.) and the Canadian Institutes of Health Research (P.A.G.) (219765). We thank Dr. Christine Smyth of the Children's Medical Research Institute Flow Cytometry Facility and Dr. Laurence Cantrill of the Westmead Core Microscopy Facility for their technical assistance. Tissues and samples were provided from the Australian Breast Cancer Tissue Bank, supported by the National Health and Medical Research Council of Australia, The Cancer Institute NSW and the National Breast Cancer Foundation. We are grateful for reagents from Prof Jenny Byrne (breast cancer cell lines) and A/Prof Aaron Schindeler (ERK antibodies) from the Children's Hospital at Westmead.

Abbreviations

DOCs	double C2-like-domain-containing proteins
SLPs	synaptotagmin-like proteins
ERK	extracellular-signal-regulated kinase
pERK	phosphorylated ERK
MAPK	mitogen-activated protein kinase
DYSF	dysferlin
MYOF	myoferlin
OTOF	otoferlin
CAPN1	calpain-1
CAPN2	calpain-2
CAPNS1	calpain small subunit-1

KD	knock-down
KO	knockout
LV	lenti virus

References

1. Britton S, Freeman T, Vafiadaki E, Keers S, Harrison R, Bushby K, Bashir R. The third human FER-1-like protein is highly similar to dysferlin. Genomics. 2000; 68:313–321. [PubMed: 10995573]
2. Lek A, Lek M, North KN, Cooper ST. Phylogenetic analysis of ferlin genes reveals ancient eukaryotic origins. BMC Evol Biol. 2010; 10:231. [PubMed: 20667140]
3. Clark JD, Lin LL, Kriz RW, Ramesha CS, Sultzman LA, Lin AY, Milona N, Knopf JL. A novel arachidonic acid-selective cytosolic PLA2 contains a Ca(2+)-dependent translocation domain with homology to PKC and GAP. Cell. 1991; 65:1043–1051. [PubMed: 1904318]
4. Nalefski EA, Falke JJ. The C2 domain calcium-binding motif: structural and functional diversity. Protein Sci. 1996; 5:2375–2390. [PubMed: 8976547]
5. Martens S, McMahon HT. Mechanisms of membrane fusion: disparate players and common principles. Nat Rev Mol Cell Biol. 2008; 9:543–556. [PubMed: 18496517]
6. Bashir R, Britton S, Strachan T, Keers S, Vafiadaki E, Lako M, Richard I, Marchand S, Bourg N, Argov Z, Sadeh M, Mahjneh I, Marconi G, Passos-Bueno MR, Moreira ED, Zatz M, Beckmann JS, Bushby K. A gene related to *Caenorhabditis elegans* spermatogenesis factor fer-1 is mutated in limb-girdle muscular dystrophy type 2B. Nat Genet. 1998; 20:37–42. [PubMed: 9731527]
7. Liu J, Aoki M, Illa I, Wu C, Fardeau M, Angelini C, Serrano C, Urtizberea JA, Hentati F, Hamida MB, Bohlega S, Culper EJ, Amato AA, Bossie K, Oeltjen J, Bejaoui K, McKenna-Yasek D, Hosler BA, Schurr E, Arahata K, de Jong PJ, Brown RH Jr. Dysferlin, a novel skeletal muscle gene, is mutated in Miyoshi myopathy and limb girdle muscular dystrophy. Nat Genet. 1998; 20:31–36. [PubMed: 9731526]
8. Bansal D, Miyake K, Vogel SS, Groh S, Chen CC, Williamson R, McNeil PL, Campbell KP. Defective membrane repair in dysferlin-deficient muscular dystrophy. Nature. 2003; 423:168–172. [PubMed: 12736685]
9. Yasunaga S, Grati M, Cohen-Salmon M, El-Amraoui A, Mustapha M, Salem N, El-Zir E, Loiselet J, Petit C. A mutation in OTOF, encoding otoferlin, a FER-1-like protein, causes DFNB9, a nonsyndromic form of deafness. Nat Genet. 1999; 21:363–369. [PubMed: 10192385]
10. Yasunaga S, Petit C. Physical map of the region surrounding the OTOFERLIN locus on chromosome 2p22-p23. Genomics. 2000; 66:110–112. [PubMed: 10843812]
11. Roux I, Safieddine S, Nouvian R, Grati M, Simmler MC, Bahloul I, Perfettini I, Le Gall M, Rostaing P, Hamard G, Triller A, Avan P, Moser T, Petit C. Otoferlin, defective in a human deafness form, is essential for exocytosis at the auditory ribbon synapse. Cell. 2006; 127:277–289. [PubMed: 17055430]
12. Pangrsic T, Lasarow L, Reuter K, Takago H, Schwander M, Riedel D, Frank T, Tarantino LM, Bailey JS, Strenzke N, Brose N, Muller U, Reisinger E, Moser T. Hearing requires otoferlin-dependent efficient replenishment of synaptic vesicles in hair cells. Nat Neurosci. 2010; 13:869–876. [PubMed: 20562868]
13. Amatschek S, Koenig U, Auer H, Steinlein P, Pacher M, Gruenfelder A, Dekan G, Vogl S, Kubista E, Heider KH, Stratowa C, Schreiber M, Sommergruber W. Tissue-wide expression profiling using cDNA subtraction and microarrays to identify tumor-specific genes. Cancer Res. 2004; 64:844–856. [PubMed: 14871811]
14. Wang WS, Liu XH, Liu LX, Lou WH, Jin DY, Yang PY, Wang XL. iTRAQ-based quantitative proteomics reveals myoferlin as a novel prognostic predictor in pancreatic adenocarcinoma. J Proteome. 2013; 91:453–465.

15. Turtoi A, Blomme A, Bellahcene A, Gilles C, Hennequiere V, Peixoto P, Bianchi E, Noel A, De Pauw E, Lifrange E, Delvenne P, Castronovo V. Myoferlin is a key regulator of EGFR activity in breast cancer. Cancer Res. 2013
16. Leung C, Yu C, Lin MI, Tognon C, Bernatchez P. Expression of myoferlin in human and murine carcinoma tumors: role in membrane repair, cell proliferation, and tumorigenesis. Am J Pathol. 2013; 182:1900–1909. [PubMed: 23499551]
17. Volakis LI, Li R, Ackerman WE, Mihai C, Bechel M, Summerfield TL, Ahn CS, Powell HM, Zielinski R, Rosol TJ, Ghadiali SN, Kniss DA. Loss of myoferlin redirects breast cancer cell motility towards collective migration. PLoS One. 2014; 9
18. Eisenberg MC, Kim Y, Li R, Ackerman WE, Kniss DA, Friedman A. Mechanistic modeling of the effects of myoferlin on tumor cell invasion. Proc Natl Acad Sci U S A. 2011; 108:20078–20083. [PubMed: 22135466]
19. Bernatchez PN, Acevedo L, Fernandez-Hernando C, Murata T, Chalouni C, Kim J, Erdjument-Bromage H, Shah V, Gratton JP, McNally EM, Tempst P, Sessa WC. Myoferlin regulates vascular endothelial growth factor receptor-2 stability and function. J Biol Chem. 2007; 282:30745–30753. [PubMed: 17702744]
20. Bernatchez PN, Sharma A, Kodaman P, Sessa WC. Myoferlin is critical for endocytosis in endothelial cells. Am J Phys Cell Phys. 2009; 297:C484–C492.
21. Demonbreun AR, Posey AD, Heretis K, Swaggart KA, Earley JU, Pytel P, McNally EM. Myoferlin is required for insulin-like growth factor response and muscle growth. FASEB J. 2010; 24:1284–1295. [PubMed: 20008164]
22. Fahmy K, Gonzalez A, Arafa M, Peixoto P, Bellahcene A, Turtoi A, Delvenne P, Thiry M, Castronovo V, Peulen O. Myoferlin plays a key role in VEGFA secretion and impacts tumor-associated angiogenesis in human pancreas cancer. Int J Cancer. 2016; 138:652–663. [PubMed: 26311411]
23. Normanno N, De Luca A, Bianco C, Strizzi L, Mancino M, Maiello MR, Carotenuto A, De Feo G, Caponigro F, Salomon DS. Epidermal growth factor receptor (EGFR) signaling in cancer. Gene. 2006; 366:2–16. [PubMed: 16377102]
24. Roberts PJ, Der CJ. Targeting the Raf-MEK-ERK mitogen-activated protein kinase cascade for the treatment of cancer. Oncogene. 2007; 26:3291–3310. [PubMed: 17496923]
25. Daughaday WH, Deuel TF. Tumor secretion of growth factors. Endocrinol Metab Clin N Am. 1991; 20:539–563.
26. Lek A, Evesson FJ, Lemckert FA, Redpath GM, Lueders AK, Turnbull L, Whitchurch CB, North KN, Cooper ST. Calpains, cleaved mini-dysferlinC72, and L-type channels underpin calcium-dependent muscle membrane repair. J Neurosci. 2013; 33:5085–5094. [PubMed: 23516275]
27. Redpath GM, Woolger N, Piper AK, Lemckert FA, Lek A, Greer PA, North KN, Cooper ST. Calpain cleavage within dysferlin exon 40a releases a synaptotagmin-like module for membrane repair. Mol Biol Cell. 2014; 25:3037–3048. [PubMed: 25143396]
28. Li R, Ackerman WEt, Mihai C, Volakis LI, Ghadiali S, Kniss DA. Myoferlin depletion in breast cancer cells promotes mesenchymal to epithelial shape change and stalls invasion. PLoS One. 2012; 7:e39766. [PubMed: 22761893]
29. Balasubramanian A, Kawahara G, Gupta VA, Rozkalne A, Beauvais A, Kunkel LM, Gussoni E. Fam65b is important for formation of the HDAC6-dysferlin protein complex during myogenic cell differentiation. FASEB J. 2014; 28:2955–2969. [PubMed: 24687993]
30. Blomme A, Costanza B, de Tullio P, Thiry M, Van Simaeys G, Boutry S, Doumont G, Di Valentin E, Hirano T, Yokobori T, Gofflot S, Peulen O, Bellahcene A, Sherer F, Le Goff C, Cavalier E, Mouithys-Mickalad A, Jouret F, Cusumano PG, Lifrange E, Muller RN, Goldman S, Delvenne P, De Pauw E, Nishiyama M, Castronovo V, Turtoi A. Myoferlin regulates cellular lipid metabolism and promotes metastases in triple-negative breast cancer. Oncogene. 2016
31. Mandic A, Viktorsson K, Strandberg L, Heiden T, Hansson J, Linder S, Shoshan MC. Calpain-mediated bid cleavage and calpain-independent Bak modulation: two separate pathways in cisplatin-induced apoptosis. Mol Cell Biol. 2002; 22:3003–3013. [PubMed: 11940658]

32. Goulet B, Baruch A, Moon NS, Poirier M, Sansregret LL, Erickson A, Bogyo M, Nepveu A. A cathepsin L isoform that is devoid of a signal peptide localizes to the nucleus in S phase and processes the CDP/Cux transcription factor. Mol Cell. 2004; 14:207–219. [PubMed: 15099520]
33. Larkin MA, Blackshields G, Brown NP, Chenna R, McGettigan PA, McWilliam H, Valentin F, Wallace IM, Wilm A, Lopez R, Thompson JD, Gibson TJ, Higgins DG. Clustal W and Clustal X version 2.0. Bioinformatics. 2007; 23:2947–2948. [PubMed: 17846036]
34. Liu Z, Cao J, Gao X, Ma Q, Ren J, Xue Y. GPS-CCD: a novel computational program for the prediction of calpain cleavage sites. PLoS One. 2011; 6:e19001. [PubMed: 21533053]
35. Webb B, Sali A. Comparative protein structure modeling using MODELLER. Curr Protoc Bioinformatics. 2014; 47(5–6):1–32. [PubMed: 25199789]
36. Arthur JSC, Elce JS, Hegadorn C, Williams K, Greer PA. Disruption of the murine calpain small subunit gene, Capn4: calpain is essential for embryonic development but not for cell growth and division. Mol Cell Biol. 2000; 20:4474–4481. [PubMed: 10825211]
37. Goll DE, Thompson VF, Li H, Wei W, Cong J. The calpain system. Physiol Rev. 2003; 83:731–801. [PubMed: 12843408]
38. Glading A, Chang P, Lauffenburger DA, Wells A. Epidermal growth factor receptor activation of calpain is required for fibroblast motility and occurs via an ERK/MAP kinase signaling pathway. J Biol Chem. 2000; 275:2390–2398. [PubMed: 10644690]
39. Shiraha H, Glading A, Chou J, Jia Z, Wells A. Activation of m-calpain (calpain II) by epidermal growth factor is limited by protein kinase A phosphorylation of m-calpain. Mol Cell Biol. 2002; 22:2716–2727. [PubMed: 11909964]
40. Glading A, Bodnar RJ, Reynolds IJ, Shiraha H, Satish L, Potter DA, Blair HC, Wells A. Epidermal growth factor activates m-calpain (calpain II), at least in part, by extracellular signal-regulated kinase-mediated phosphorylation. Mol Cell Biol. 2004; 24:2499–2512. [PubMed: 14993287]
41. Franco SJ, Huttenlocher A. Regulating cell migration: calpains make the cut. J Cell Sci. 2005; 118:3829–3838. [PubMed: 16129881]
42. Turk D, Podobnik M, Popovic T, Katunuma N, Bode W, Huber R, Turk V. Crystal structure of cathepsin B inhibited with CA030 at 2.0-A resolution: a basis for the design of specific epoxysuccinyl inhibitors. Biochemistry. 1995; 34:4791–4797. [PubMed: 7718586]
43. Tan GJ, Peng ZK, Lu JP, Tang FQ. Cathepsins mediate tumor metastasis. World J Biol Chem. 2013; 4:91–101. [PubMed: 24340132]
44. Wang KK. Calpain and caspase: can you tell the difference? Trends Neurosci. 2000; 23:20–26. [PubMed: 10631785]
45. Cooper ST, Kizana E, Yates JD, Lo HP, Yang N, Wu ZH, Alexander IE, North KN. Dystrophinopathy carrier determination and detection of protein deficiencies in muscular dystrophy using lentiviral MyoD-forced myogenesis. Neuromuscul Disord. 2007; 17:276–284. [PubMed: 17303423]
46. Gauster M, Siwetz M, Orendi K, Moser G, Desoye G, Huppertz B. Caspases rather than calpains mediate remodelling of the fodrin skeleton during human placental trophoblast fusion. Cell Death Differ. 2010; 17:336–345. [PubMed: 19798107]
47. Fox JE, Reynolds CC, Morrow JS, Phillips DR. Spectrin is associated with membrane-bound actin fllaments in platelets and is hydrolyzed by the Ca^{2+}-dependent protease during platelet activation. Blood. 1987; 69:537–545. [PubMed: 3026523]
48. Harris AS, Morrow JS. Calmodulin and calcium-dependent protease I coordinately regulate the interaction of fodrin with actin. Proc Natl Acad Sci U S A. 1990; 87:3009–3013. [PubMed: 2326262]
49. Maravei DV, Trbovich AM, Perez GI, Tilly KI, Banach D, Talanian RV, Wong WW, Tilly JL. Cleavage of cytoskeletal proteins by caspases during ovarian cell death: evidence that cell-free systems do not always mimic apoptotic events in intact cells. Cell Death Differ. 1997; 4:707–712. [PubMed: 16465283]
50. Lostal W, Bartoli M, Roudaut C, Bourg N, Krahn M, Pryadkina M, Borel P, Suel L, Roche JA, Stockholm D, Bloch RJ, Levy N, Bashir R, Richard I. Lack of correlation between outcomes of membrane repair assay and correction of dystrophic changes in experimental therapeutic strategy in Dysferlinopathy. PLoS One. 2012; 7

51. Sebolt-Leopold JS, Herrera R. Targeting the mitogen-activated protein kinase cascade to treat cancer. Nat Rev Cancer. 2004; 4:937–947. [PubMed: 15573115]

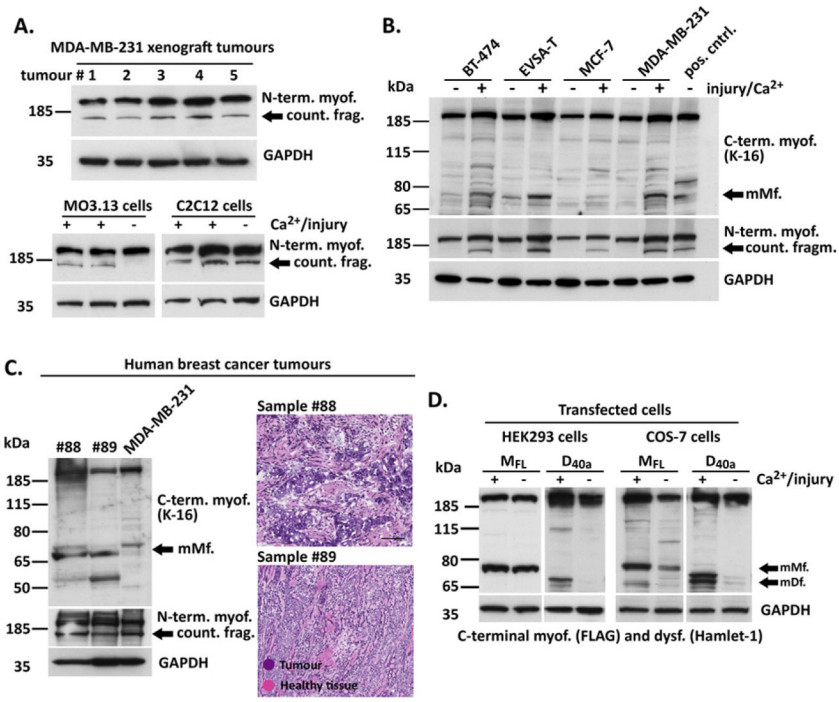

Fig. 1.

Myoferlin cleavage products are detected in breast tumours, breast cancer cell lines and transfected cells. **(A)** Western blot analysis of five mouse xenograft tumour samples derived from MDA-MB-231 cells transplanted into nude mice, showing an N-terminal myoferlin cleavage product. **(B)** Western blot analysis of endogenous myoferlin in four different human breast cancer cell lines (BT-474, EVSA-T, MCF-7 and MDA-MB-231) with (+) or without (−) scrape-injury in $+Ca^{2+}$-PBS. A ~75kDa C-terminal cleavage product is detected with the K-16 antibody recognizing a C-terminal myoferlin epitope, and a ~180 kDa counter fragment detected with 7D2 that recognizes an N-terminal myoferlin epitope. K16 works less effectively than 7D2 with a higher background, thus 30 μg total protein is loaded on K16 gel and 10 μg total protein loaded on the 7D2 gel. **(C)** ~75 kDa C-terminal myoferlin fragments (doublet bands) and an ~180 N-terminal counter fragment are also detected in triple negative human breast cancer samples (#88 and #89). H&E staining of fresh frozen tumour sections of the same samples run on the western blot. The purple stain represents tumour tissue and the pink stain normal breast tissue (H&E staining provided by the ABCTB). Scale bar 500 μm. **(D)** Western blot analysis of HEK293 and COS-7 cells transfected with full length myoferlin (M_{FL}) or dysferlin containing the calpain cleavage site in exon 40a (D_{40a}) with (+) or without (−) scrape-injury in $+Ca^{2+}$-PBS.

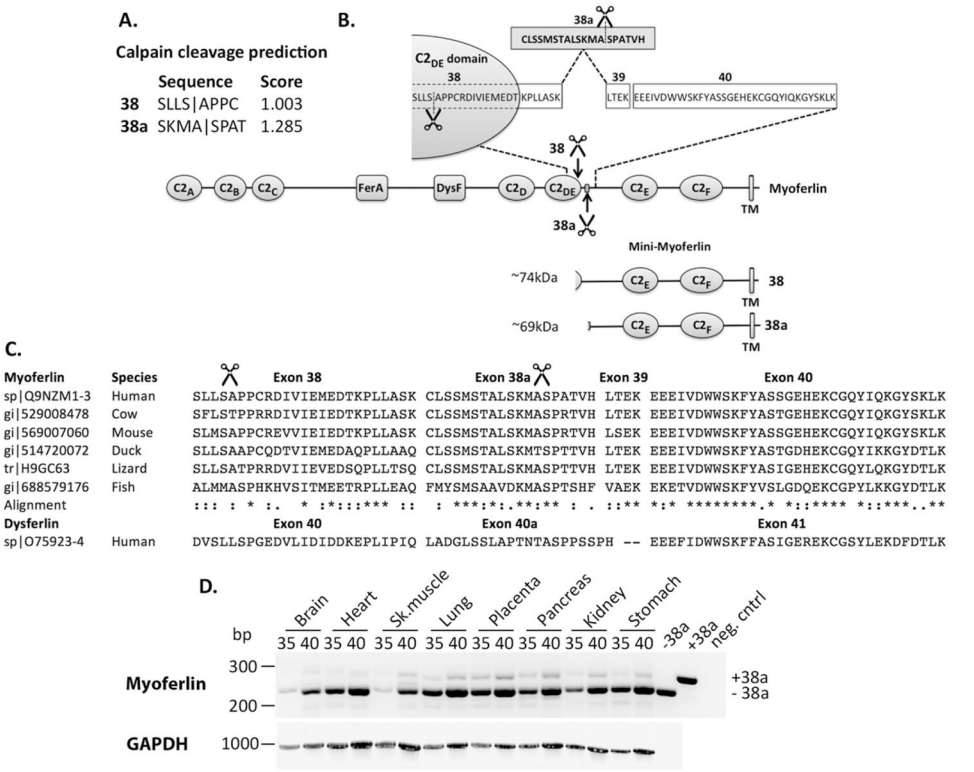

Fig. 2.

Myoferlin bears two predicted calpain cleavage sites. **(A)** Calpain cleavage prediction (GPS-CCD, ccd.biocuckoo.org; [29]) of myoferlin resulted in two highly predicted cleavage sites consistent with production of a 75–80 kDa C-terminal cleavage fragment. **(B)** Schematic of the myoferlin protein structure showing the location of the two predicted calpain cleavage sites. The first predicted cleavage site (SLLS|APPC) is encoded by constitutive in exon 38, at the end of the $C2_{DE}$ domain and would result in a ~74 kDa mini-myoferlin fragment. The second predicted cleavage site (SKMA|SPAT) is encoded by alternatively spliced exon 38a in the linker directly adjacent to $C2_{DE}$, which would result in a slightly smaller mini-myoferlin (~69 kDa). **(C)** Phylogenetic amino acid sequence alignment showing that exon 38a is evolutionary conserved down to the fish class, and that myoferlin exon 38a aligns to the same position as exon 40a in dysferlin. **(D)** PCR analysis of human tissue cDNA showing myoferlin RNA is expressed throughout the different tissues tested and reveals that exon 38a is expressed as a minor species in human tissues (~10% of total transcripts). PCR amplification was performed for 35 and 40 cycles to control for saturation. +38a and -38a are plasmid controls with and without exon 38a.

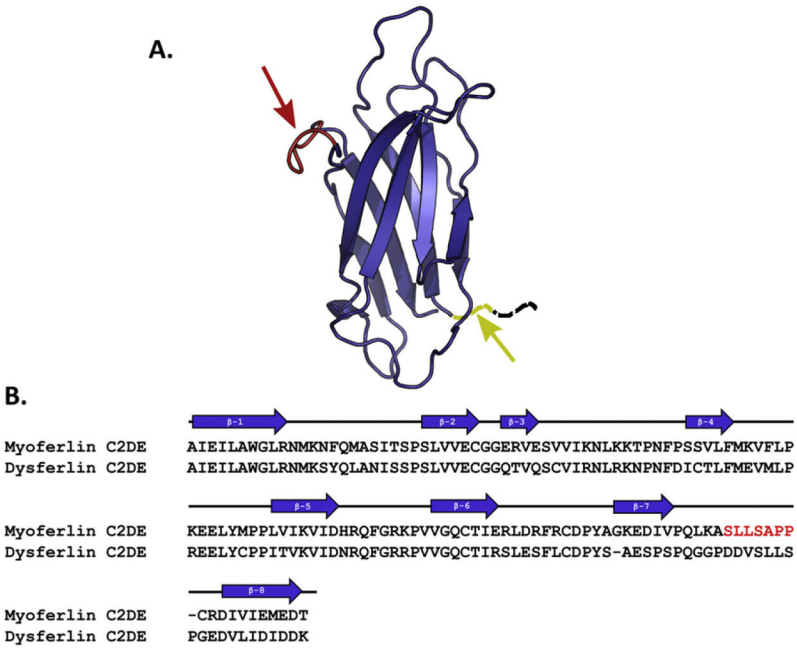

Fig. 3.

Molecular modelling of predicted calpain cleavage sites in myoferlin. **(A)** Homology modelling of the $C2_{DE}$ domain of myoferlin based on the closest solved crystal structure of myoferlin $C2_A$ (2DMH, see methods) indicates the first cleavage site (encoded by exon 38, red arrow) is located in a loop between the last two beta strands (β7 and β8) of myoferlin $C2_{DE}$ (red loop). The cleavage site in exon 38a (yellow arrow) is located in the linker region (dashed line) that cannot be modelled and was drawn freely onto the model (yellow dashed line). **(B)** Alignment of the $C2_{DE}$ sequence of dysferlin and myoferlin in relation to the β-strand (purple) shows that the region of the first cleavage site of myoferlin has the least homology between dysferlin and myoferlin.

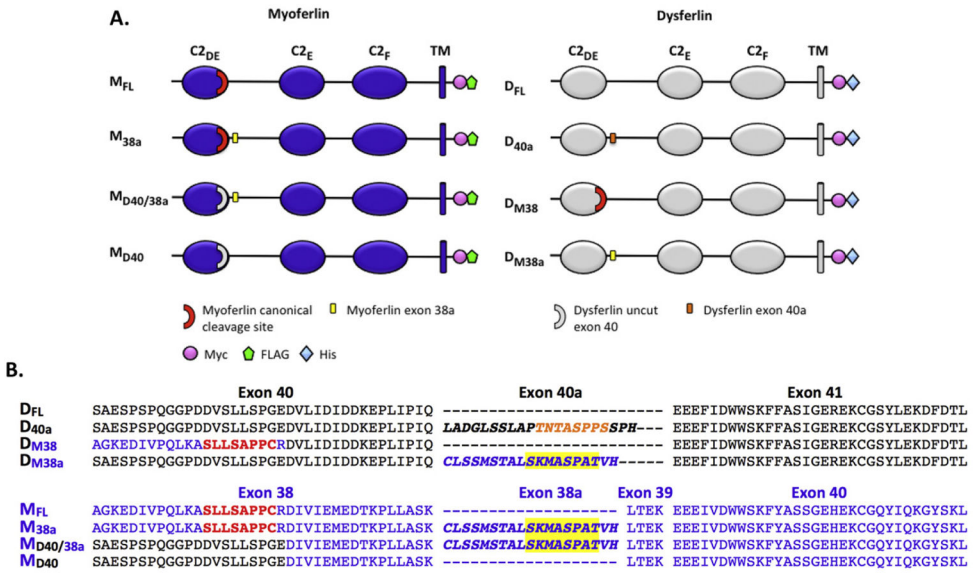

Fig. 4.

Chimeric constructs of myoferlin and dysferlin. **(A)** Graphical illustration of the design of chimeric expression constructs. Myoferlin sequence is displayed in purple and dysferlin sequence in grey scale. The first predicted calpain cleavage site (SLLS|APPC) site in myoferlin is coloured in red and the second cleavage site in exon 38a is highlighted in yellow (SKMA|SPAT). The cleavage site in exon 40a in dysferlin is coloured in orange (TNTA|SPPS). **(B)** Amino acid sequences of the chimeric constructs. To confirm the cleavage site in myoferlin resided within the non-conserved loop between the 7th and 8th β-strand of the $C2_{DE}$ domain (see schematic in Fig. 3), we reciprocally substituted residues comprising the 7th and 8th β-strand and intervening linker $C2_{DE}$ between dysferlin and myoferlin (D_{M38} and M_{D40}).

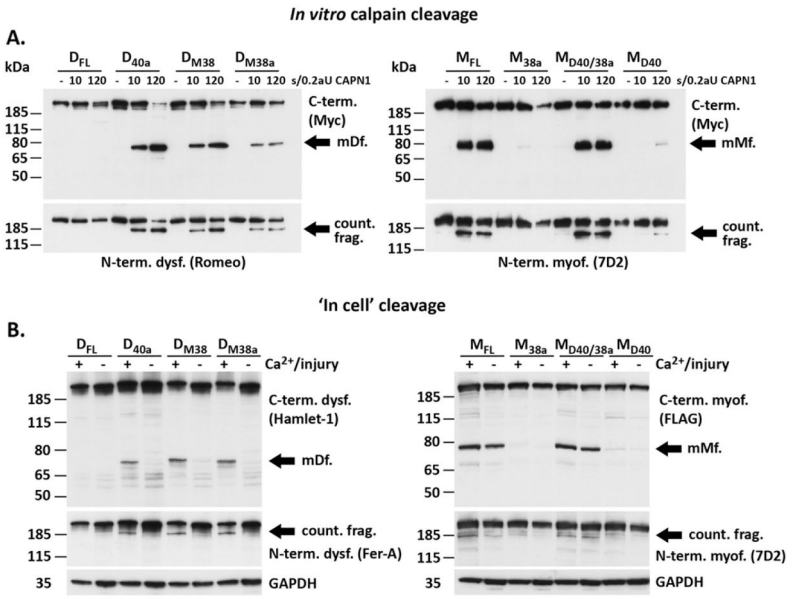

Fig. 5.

Evaluation of predicted calpain-cleavage sites in myoferlin. **A)** *In vitro* cleavage of dysferlin and myoferlin constructs immunopurified from transfected HEK293 cells and incubated with recombinant calpain-1. Protein-bound Sepharose beads were incubated in buffer containing 2 mM $CaCl_2$ in the presence of purified 0.2 A.U. of recombinant calpain-1 at 30 °C for 10 or 120 s, or in the absence of calpain (−). Proteolysis was rapidly inhibited by reconstitution of the reaction in SDS lysis buffer and heating to 94 °C. Digested samples were analyzed by SDS–PAGE and western blot. **B**) *In cell* cleavage of dysferlin and myoferlin expression constructs is induced *via* scrape-harvesting of transfected HEK293 cells. (+) with scrape injury in $+Ca^{2+}$- PBS; (−) without scrape injury, harvested directly into ice-cold RIPA buffer with EDTA. Dysferlin without a calpain cleavage site (D_{FL}) is not cleaved. Dysferlin with exon 40a (D_{40a}) is cleaved by recombinant calpain (A) and during scrape-harvesting (B). Both predicted myoferlin cleavage sites in exon 38 and exon 38a can functionally substitute for exon 40a in *in vitro* and *in cell* cleavage assays (D_{M38}, D_{M38a}). Myoferlin (M_{FL}) is cleaved by calpain-1 *in vitro* (A) and is cleaved independently of scrape injury in transfected HEK293 (B). Substitution of myoferlin exon 38 with the corresponding residues from dysferlin (encoded by exon 40; M_{D40}) prevents cleavage, confirming myoferlin exon 38 sequences contain a cleavage motif. Paradoxically, myoferlin constructs with exon 38a (M_{38a}) are not cleaved *in vitro* or *in cells*. Inclusion of exon 38a sequences regulates (precludes) cleavage both within exon 38a as well as at the exon 38 site.

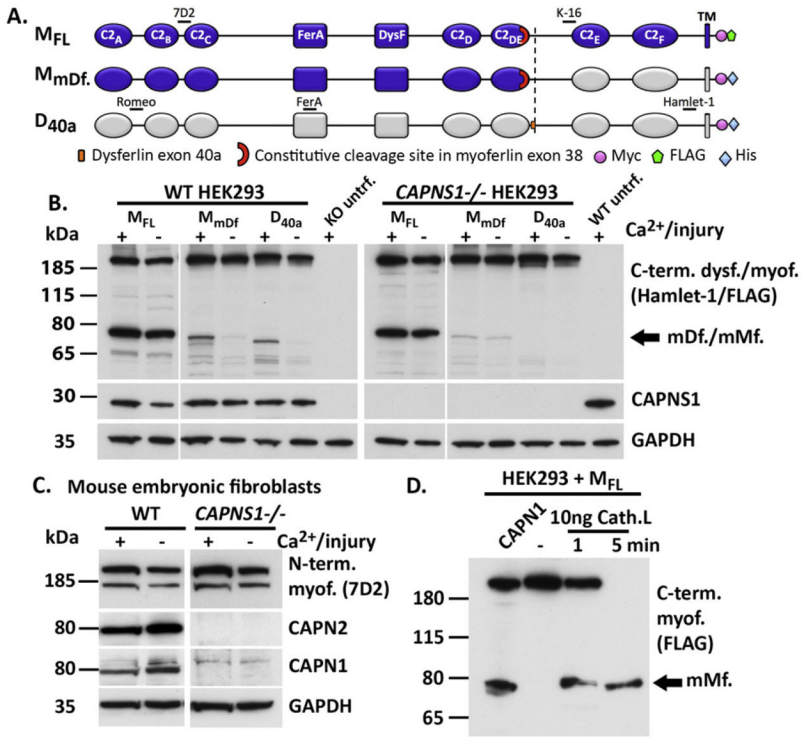

Fig. 6.

Myoferlin cleavage is independent of calpain-1 and -2. The dysferlin C-terminal domain confers calpain- and Ca^{2+}-dependent cleavage on myoferlin. **(A)** Illustration of expression constructs; Full lengthMyoferlin(M_{FL}),Dysferlinwith exon40a (D_{40a}),Myoferlin with mini-dysferlin$_{C72}$ C-terminal domains (M_{mDf}). Antibody epitopes and epitope tags are annotated for each construct. **(B)**Western blot analysis of HEK293 cells(WT and C*APNS1*$^{-/-}$) transfected with M_{FL},M_{mDf}, and D_{40a}, or an untransfected control. In contrast to D_{40a}, proteolytic cleavage of M_{FL} is insensitive to targeted knock-out of CAPNS1, and does not require scrape injury. Substitution of the myoferlin C-terminus for the dysferlin C-terminal domains confers calpain-dependent, injury-dependent cleavage on M_{mDf}. **(C)** WT and *CAPNS1*$^{-/-}$ mouse embryonic fibroblasts (MEFs) showing cleavage of endogenous myoferlin detectable with the N-terminal antibody (7D2). **(D)** *In vitro* cathepsin L cleavage of M_{FL} transfected HEK293 cells shows the release of the same mini-myoferlin seen with the *in vitro* calpain-1 cleavage.

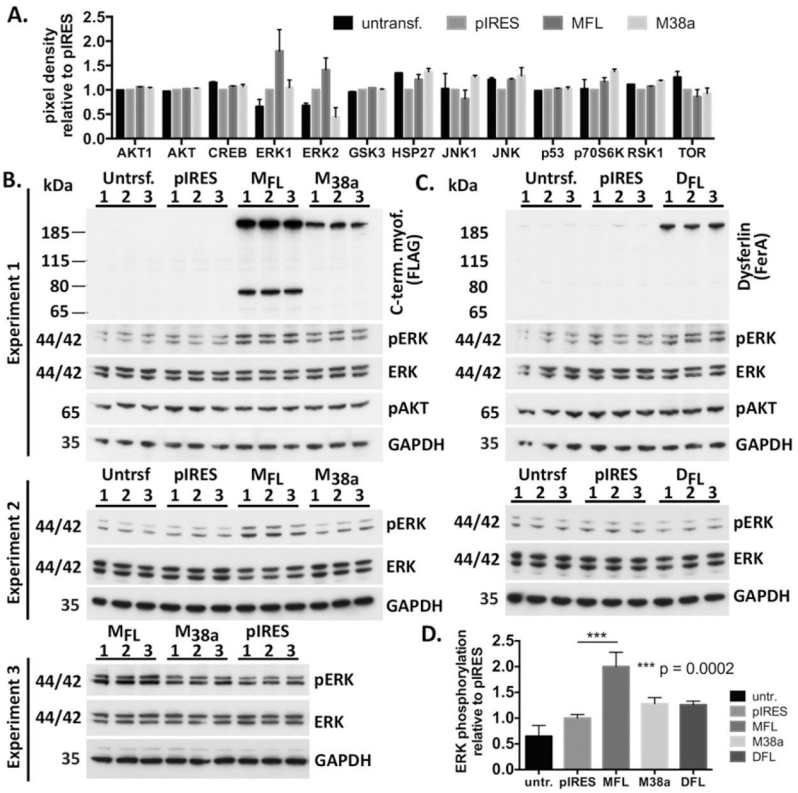

Fig. 7.

Overexpression of canonical full-length myoferlin (MFL) but not the uncleavable M38a, upregulates phosphorylated ERK in transfected HEK293 cells. **(A)** Cell lysates from transfected HEK293 cells were incubated with Proteome Profiler™ Antibody Arrays (Human Phospho-MAPK and Mouse-RTK Array Kit, R&D systems). Histogram of densitometry from duplicate spots of 13 representative proteins from the Human Phospho-MAPK Array showing elevation of phospho-ERK. No differences between M_{FL} and M_{38a} or empty pIRES were observed for the remaining phosphoproteins (not shown). **(B and C)** Western blot experiments confirm specific upregulation of pERK relative to total ERK in HEK293 cells transfected with M_{FL}, but not M_{38a}, D_{40a} or empty pIRES. Levels of pAKT were unchanged. Data show three experiments performed in triplicate. **(D)** Densitometric analysis of combined data from western blots showing up-regulation of pERK in M_{FL} expressing HEK293 cells was significantly elevated relative to pIRES expressing cells (p = 0.0002) (one way ANOVA, Prism 6).